

Article

Hydrophobic Deep Eutectic Solvents for the Recovery of Bio-Based Chemicals: Solid–Liquid Equilibria and Liquid–Liquid Extraction

Thomas Brouwer , Bas C. Dielis, Jorrit M. Bock and Boelo Schuur *

Faculty of Science and Technology, Sustainable Process Technology Group, University of Twente, Drienerlolaan 5, Meander Building 221, 7522 NB Enschede, The Netherlands; t.brouwer@utwente.nl (T.B.);

b.c.dielis@student.utwente.nl (B.C.D.); j.m.bock@student.utwente.nl (J.M.B.)

* Correspondence: b.schuur@utwente.nl; Tel.: +31-53-489-2891

Abstract: The solid–liquid equilibrium (SLE) behavior and liquid–liquid extraction (LLX) abilities of deep eutectic solvents (DESs) containing (a) thymol and L-menthol, and (b) trioctylphosphine oxide (TOPO) and L-menthol were evaluated. The distribution coefficients (K_D) were determined for the solutes relevant for two biorefinery cases, including formic acid, levulinic acid, furfural, acetic acid, propionic acid, butyric acid, and L-lactic acid. Overall, for both cases, an increasing K_D was observed for both DESs for acids increasing in size and thus hydrophobicity. Furfural, being the most hydrophobic, was seen to extract the highest K_D (for DES (a) 14.2 ± 2.2 and (b) 4.1 ± 0.3), and the K_D of lactic acid was small, independent of the DESs (DES (a) 0.5 ± 0.07 and DES (b) 0.4 ± 0.05). The K_D of the acids for the TOPO and L-menthol DES were in similar ranges as for traditional TOPO-containing composite solvents, while for the thymol/L-menthol DES, in the absence of the Lewis base functionality, a smaller K_D was observed. The selectivity of formic acid and levulinic acid separation was different for the two DESs investigated because of the acid–base interaction of the phosphine group. The thymol and L-menthol DES was selective towards levulinic acid ($S_{ij} = 9.3 \pm 0.10$, and the TOPO and L-menthol DES was selective towards FA ($S_{ij} = 2.1 \pm 0.28$).

Keywords: L-menthol; deep eutectic solvent; bio-refinery; carboxylic acids; furfural



Citation: Brouwer, T.; Dielis, B.C.; Bock, J.M.; Schuur, B. Hydrophobic Deep Eutectic Solvents for the Recovery of Bio-Based Chemicals: Solid–Liquid Equilibria and Liquid–Liquid Extraction. *Processes* **2021**, *9*, 796. <https://doi.org/10.3390/pr9050796>

Academic Editor: Guilhem Arrachart

Received: 12 April 2021

Accepted: 29 April 2021

Published: 30 April 2021

Publisher's Note: MDPI stays neutral with regard to jurisdictional claims in published maps and institutional affiliations.



Copyright: © 2021 by the authors. Licensee MDPI, Basel, Switzerland. This article is an open access article distributed under the terms and conditions of the Creative Commons Attribution (CC BY) license (<https://creativecommons.org/licenses/by/4.0/>).

1. Introduction

It is estimated that in the chemical industry, about 20 million metric tons of organic solvents are produced annually [1]. These solvents are essential in chemical processes in order to facilitate desired outcomes including separations. However, excessive use of toxic, non-renewable solvents can be detrimental to the environment and have subsequent adverse consequences for future generations. In line with the global sustainable development goals, defined in the Brundtland Report as “development that meets the needs of the present without compromising the ability of future generations to meet their own needs”, solvents should be considered that have a low impact on the environment and society [2]. For this reason, the search to identify newly sustainable, bio-derived, organic solvents is of the utmost importance.

One promising sustainable feedstock is (lignocellulosic) biomass, in which polymeric sugar chains, e.g., cellulose and hemicellulose, and lignin can be converted into a great variety of chemicals [3]. This can be done either by hydrolysis [4–7], fermentation [8–10], or combinations thereof (enzymatic hydrolysis) [11,12]. Typical hydrolysis products [4,7,13] include formic acid, levulinic acid, and furfural, formed via sugars and 5-hydroxymethylfurfural, while products from fermentation can be acetic acid [14,15], propionic acid [14,15], butyric acid [14,15], and L-lactic acid [14–16], but valeric acid [17], caproic acid [17], succinic acid [16,18], itaconic acid [16], mandelic acid [16], and alcohols [15] are also known to be produced.

For the isolation of the produced chemicals, extraction is often proposed, as products are often available in low concentrations in aqueous media. Hence, in situ reactive extractions using Aliquat 336 and TOPO dissolved in methyloctanoate [19] or trioctylamine (TOA) in oleyl alcohol [20] are proposed. In addition, membrane-assisted in situ reactive extraction of carboxylates from fermented wastewater has been applied using TOA in n-decanol [16]. Both intend to intensify the product formation through the in situ removal and isolation of products. Commonly used solvents for these applications include nitrogen-based extractants (e.g., TOA and Aliquat 336); phosphorus-based extractants (e.g., TOPO), which can be diluted in various hydrophobic solvents; and, more recently, ionic liquids [21].

In line with the Sustainable Development Goals, biobased solvents can be used to either replace traditional diluents while still using traditional extractants, or can completely replace the traditional extraction system. Several pathways can be chosen to search for these renewable organic solvents. A great number of organic molecules that may be applied as solvents can be derived, for instance, from biomass [22]. Numerous examples of bio-derived organic solvents that can replace traditional fossil-based organic solvents are known. Limonene (derived from citrus peel) has been shown to replace toluene in the cleaning sector [23] or to break azeotrope in the diisopropyl ether/acetone vapor-liquid equilibrium [24]; other examples of bio-based solvents are γ -valerolactone [25], 2-methyltetrahydrofuran [26], and dihydrolevoglucosenone (Cyrene) [27,28], among others [3,22].

An interesting area of solvent development was initiated by Abbot et al. [29] in 2003. They described interesting solvent properties for binary mixtures between urea and several ammonium salts that are liquid at room temperature. These mixtures were eventually named deep eutectic solvents (DES) [30]. Since then, these DESs have been used in extractive distillation [31], liquid-liquid systems [26,32,33], solid-liquid systems [34–36], and biomass fractionations [37,38], to name a few. These DESs are a promising option, as they can liquefy otherwise solid extractants (e.g., TOPO) [39] and extend the availability of possible extractant combinations [40], as was recently shown for desulfurization [41].

Four main types of DESs were first distinguished [42]: (I) a quaternary ammonium salt with a metal chloride, (II) a quaternary ammonium salt with a metal chloride hydrate, (III) a quaternary ammonium salt with a hydrogen bond donor, and (IV) a metal chloride hydrate with a hydrogen bond donor. Most DESs contain ionic species and strong hydrogen bonds are present. This makes many DESs quite hygroscopic [43], and this limits their applicability in biorefinery applications where aqueous streams are common. Hence, hydrophobic DESs were sought after when extractions from aqueous streams are aimed at and found by, among others, van Osch et al. [44], who used high-molecular weight carboxylic acids; Gilmore et al. [45] and Schaeffer et al. [46], who used trioctylphosphine oxide (TOPO); Cañadas et al. [47] who used high-molecular amines; and Abranches et al. [48], who demonstrated an unusually strong interaction between aromatic and aliphatic hydroxyl groups and defined this as a type V non-ionic DES. The hydrophobic DESs described by van Osch et al. [44] have been studied in liquid-liquid extractions [44,49,50], and hydrophobic DESs, in general, have been applied to remove riboflavin [51], chlorophenols [52], caffeine [53], tryptophan [53], vanillin [53], isophthalic acid [53], platinum group and transition metals [45,46], phenolic antioxidants [47], and polycyclic aromatic hydrocarbons [54] from water.

In this work, a type V DES based on L-menthol and thymol, as shown by Abranches et al. [48], or a TOPO and L-menthol DES, inspired by Gilmore et al. [45] and Schaeffer et al. [46], was applied to two bio refinery-relevant liquid-liquid extractions. Case I is the hydrolysis of lignocellulosic materials followed by an acid-catalyzed conversion of hexose and pentose sugars, which produces platform chemicals, such as levulinic acid, formic acid, and furfural [5,6,55]. The separation case involves the separation of formic acid and levulinic acid. Case II is the fermentation of wastewater, which produced volatile fatty acids such as acetic acid, propionic acid, and butyric acid, as well as lactic acid [14,56,57]. These acids then needed to be removed from the fermented wastewater and be fractionated, which

was investigated through liquid–liquid extraction (LLX) with the two DESs. Before the extraction assessments, the solid–liquid equilibria (SLE) were determined to establish the eutectic behavior of this type of V DES. The SLE of the thymol/L-menthol was reproduced and validated against the results published by Abranches et al. [48]. This validated our measurement technique for the new system of TOPO and L-menthol. The toxicity of the extraction agents is of course important, and DESs are not necessarily less toxic than their constituents [58], although this will not be further examined in this work.

2. Materials and Methods

2.1. Materials

Chemicals, if not otherwise specified, were used as received without any additional purification. Thymol ($\geq 98.5\%$), trioctylphosphine oxide (99%), L-menthol ($\geq 99\%$), propionic acid ($\geq 99.5\%$), furfural (99%), acetic acid ($\geq 99\%$), formic acid ($\geq 96\%$), and butyric acid ($\geq 99\%$) were obtained from Sigma Aldrich, while levulinic acid (98+) was purchased from Acros. Crystalline L-lactic acid was kindly supplied by Corbion.

2.2. Experimental and Analytical Methods

2.2.1. Melt Point Determination (Cloud Point)

The cloud point method was applied to determine the melting point of the pre-defined mixtures of thymol or TOPO and L-menthol. The cloud point was the analog to the well-known dew point at which condensation occurred in the gas–liquid phase transition, although in this case, transparent liquid became cloudy as the liquid–solid phase transition occurred [59]. Each pre-defined mixture was mixed in 10 mL capped glass vials using an analytical balance with an accuracy of 0.5 mg. Each sample was placed in a temperature-controlled shaking water bath for at least 1 h at 50 °C to obtain a homogeneous liquid mixture. Each sample was cooled and solidified over at least 16 h at -20 °C, after which, at an increase of 0.4 °C/min, the cloud point was manually checked. Each determination was done in duplo, and the error bars displayed in the results corresponded to the standard deviation over the two measurements.

2.2.2. Liquid–Liquid Extraction Experiments

Each liquid–liquid extraction (LLX) experiment was conducted in a 10 mL capped glass vial after all components in both phases were weighed on an analytical scale with an accuracy of 0.5 mg. The biphasic systems in the vials were shaken rigorously using a vortex mixer and were consecutively shaken in a shaking bath for at least 20 h at a constant temperature of 25 ± 0.02 °C. The mass of the aqueous phase was kept constant at 3 g, with a solvent to feed ratio of 1 on a mass basis. The aqueous phase contained 1 wt.% of formic acid, levulinic acid, furfural, acetic acid, propionic acid, butyric acid, or L-lactic acid. The solvent (DES) phase was kept either at a 1:1 molar ratio, which is a 1:1.04 weight ratio for the thymol and L-menthol DES, or a 1:3 molar ratio, which is a 1:1.2 weight ratio for the TOPO and L-menthol DES. The color and turbidity of each biphasic aqueous DES mixture was compared before, during, and after each experiment to detect any instability. Furthermore, based on the HPLC analyses of the aqueous phases after extraction, it was additionally confirmed that the DES was stable.

2.2.3. HPLC

The aqueous phase concentrations of each solute were determined with HPLC using an Agilent 1200 series apparatus, equipped with a Hi-Plex-H column (300×7.7 mm) and a refractive index detector (RID) at 55 °C. A 5 mM aqueous sulphuric acid solution was applied as the eluent at a flow rate of 0.6 mL/min. The injection volume was 10 μ L and the column oven was isothermally operated at 65 °C. No detectable peaks were found for the thymol, TOPO, and L-menthol, and so no unidentified peaks were found, indicating a very low, negligible, solubility of these compounds, and the stability of all compounds in the biphasic aqueous DES mixture.

2.2.4. Karl Fischer Titration

The water content of the DES was analyzed with Karl Fischer Titration using a 787 KF Titrino 730 TiStand of Metrohm. A methanol/dichloromethane (volumetric ratio of 3:1) solution and HYDRANAL[®] were used as the titrant. Water contents of ~0.5 wt.% were determined in the thymol and L-menthol, and TOPO and L-menthol DESs.

2.2.5. Definitions

The liquid–liquid extractions for each of the solutes using the DES were evaluated according to their distribution coefficients (K_D), as defined in Equation (1),

$$K_{D,i} = [x_i]_{DES} / [x_i]_{aq} \quad (1)$$

where $[x_i]$ represents the concentration (mol/L) of each solute in either the DES phase or aqueous phase. Although in this work, only extractions were done with single solutes, these experiments indicate the preference of the DESs when individual distributions are compared, and in the comparison of two solutes, the selectivity (S_{ij}), as in Equation (2), was applied,

$$S_{ij} = K_{D,i} / K_{D,j} \quad (2)$$

where S_{ij} is the ratio between the distribution coefficients of compounds i and j .

The DES phase concentrations were determined using the mass balance, and taking into account the mass of water leached into the organic phase.

2.3. Modeling

The solid–liquid equilibrium of this eutectic mixture can be described by Equation (3),

$$\ln(x_i \gamma_i) = \Delta_m H / R (1/T_m - 1/T) \quad (3)$$

where x_i is the mole fraction of solute i and γ_i is the activity coefficient of this solute in the liquid phase. T is the absolute temperature, while T_m and $\Delta_m H$ are the melting temperature and the melting enthalpy of the same pure solute, respectively. Lately, R is the universal gas constant [60]. However, this is not the complete equilibrium description, as the contribution of the heat capacities is neglected [61]. Setting the γ_i to unity allows for a direct determination of the ideal solid–liquid phase equilibrium. However, this is not the case for most mixtures and the γ_i needs to be determined. This can be done experimentally by correlating the phase envelop or it can be predicted [62].

The prediction of γ_i can be done using the software package COSMO-RS, which is an abbreviation for the conductor-like screening model for real solvents [63]. This model combines initial quantum mechanical calculations with statistical thermodynamics to predict, among others, phase diagrams [64,65]. These phase diagram calculations were performed in the associated software package COSMOthermX C30_1705, with a density functional theory (DFT) with a Becke and Pedrew (BP86) functional level of theory and triple- ζ valence polarized (TZVP) basis set. The required σ -profiles required for the calculation were determined in TURBOMOLE, from the associated software package COSMOconf. Here, geometric optimizations were performed to distinguished one or multiple sets of conformers with similar energies. Manually, the $\Delta_m H$ and T_m of L-menthol (12.89 kJ/mol; 315.7 K) [48], thymol (22.01 kJ/mol; 323.5 K) [48], and TOPO (53.5 kJ/mol; 326.4 K) [39] were added to be able to predict the solid–liquid equilibria (SLE) of the chosen DESs.

The geometric optimizations confirmed a total of 6, 4, and 10 conformers for L-menthol, thymol, and TOPO, respectively. For the final solid–liquid equilibrium (SLE), the combination of conformer sets with the strongest interactions was deemed to be the most likely, and this result is shown.

3. Results

3.1. Solid–Liquid Equilibria (SLE)

The systems of L-menthol and thymol and L-menthol and TOPO were investigated for their properties when changing phase from solid to liquid. In the case of L-menthol and thymol, literature data are available from Abranches et al. [48], and a comparison of their data serves as validation for our experimental method. Figure 1 shows the corresponding solid–liquid equilibria (SLE). Our experimental results for L-menthol and thymol complies with the experimental data and COSMO-RS prediction found by Abranches et al. [48], thus confirming our method. The results also confirm the unusually strong attractive interactions between the aromatic and aliphatic hydroxyl groups, which is attributed to the resonance and sp^2 nature of the oxygen atom in the aromatic thymol [48,66]. An eutectic point at ~ 200 K was predicted using COSMO-RS at ~ 0.45 mol.% thymol, although this was not experimentally verified because of the temperature limitations of the set-up. In addition, a strong interaction between the basic phosphine oxide and the aliphatic hydroxyl group of L-menthol led to a predicted eutectic point at ~ 240 K at ~ 0.25 mol.% TOPO. However, there was a systematic deviation between the COSMO-RS prediction and the experimental data in the TOPO/L-menthol DES, which occurred at low TOPO fractions, indicating that the non-ideal effect induced by TOPO upon the L-menthol was not accurately predicted and was over predicted. This resulted in an activity coefficient lower than what was experimentally determined. Nevertheless, both DESs were therefore liquid at room temperature, which enabled their ability to be used as an extraction medium.

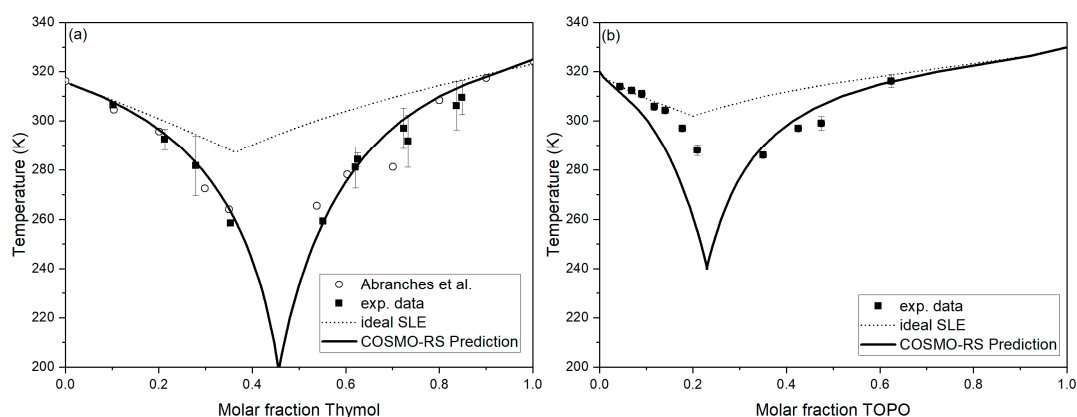


Figure 1. Experimentally determined solid–liquid equilibrium (SLE) of (a) L-menthol and thymol and (b) L-menthol and TOPO following the cloud point method. The obtained values of the L-menthol and thymol are additionally compared with those reported by Abranches et al. [48]. Additionally, the ideal SLE curve and the prediction from COSMO-RS are shown.

3.2. Liquid–Liquid Extraction (LLX)

The liquid–liquid extractions (LLX) were performed using an equimolar ratio of thymol and L-menthol, and a 1:3 molar ratio of TOPO and L-menthol. The first ratio was chosen as it was near the eutectic point prediction, as seen in Figure 1. A 1:3 molar ratio was used in the latter case, which differed from the eutectic point prediction, but this was done to obtain a more concentrated presence of the basic TOPO. In Figure 2, the distribution coefficients can be seen for all solutes in the studied cases. For Case I, it can be seen that when using the thymol and L-menthol DES, formic acid was the least extracted ($K_D = 0.090 \pm 0.004$), levulinic acid was extracted with a K_D of 0.090 ± 0.008 , and furfural was the most efficiently extracted with a K_D of 14 ± 2.2 . Oppositely, levulinic acid was less extracted ($K_D = 0.914 \pm 0.094$) than formic acid ($K_D = 1.88 \pm 0.17$) in the TOPO and L-menthol DES, while furfural was still most efficiently extracted, with a K_D of 4.07 ± 0.25 , although it was less than the thymol and L-menthol DES.

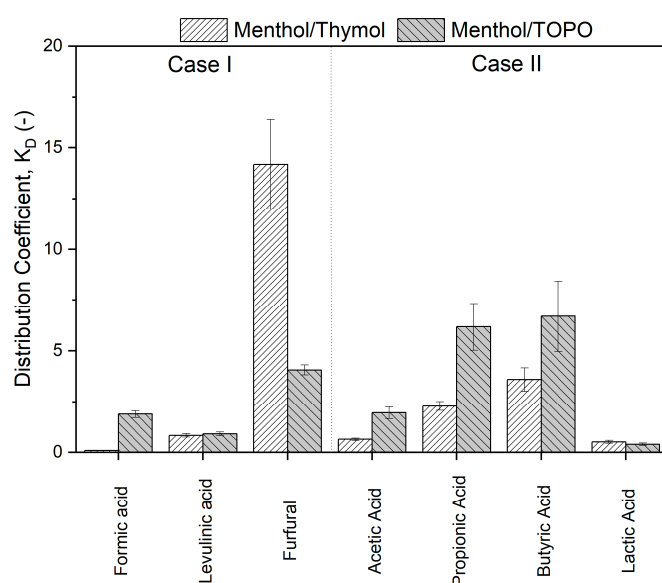


Figure 2. The distribution coefficients of formic acid, levulinic acid, and furfural (Case I), and acetic acid, propionic acid, butyric acid, and L-lactic acid (Case II). Each extraction was done with a 1:1 molar ratio of thymol and L-menthol, and a 1:3 molar ratio of TOPO and L-menthol DES at an S:F ratio of 1 (mass basis) at 25 °C. The error bars represent the combined experimental and analytical errors.

The apolar thymol and L-menthol DES contained aliphatic and aromatic hydroxyl groups able to bond with formic acid, although formic acid tends to be present as dimers [67] that rebate the interactions between the hydroxyl groups, which results in a low K_D . The more phosphine oxide group interacted with the formic acid dimer and, consequently, a (much) larger K_D was observed for the TOPO and L-menthol DES. The hydrophobic nature of furfural caused repulsive tendencies in the aqueous phase, and therefore promoted extraction towards the DES solvents, although the structurally similar thymol caused further affinity towards furfural than TOPO. Levulinic acid had a slight preference for the aqueous phase, as a result of the carboxylic and ketone function groups, although the C₅-hydrocarbon backbone still allowed for a considerable extraction in both DESs. Furfural could be removed from the aqueous mixture by hydrophobic ionic liquids [68,69] or hydrophobic organic solvents, such as p-xylene [70] or toluene [55,70]. Hence, the DES in this work allowed for either a selectivity of levulinic acid over formic acid of $S_{ij} = 9.3 \pm 0.10$ (thymol and L-menthol DES), or a selectivity of formic acid over levulinic acid of $S_{ij} = 2.1 \pm 0.28$ (TOPO and L-menthol DES).

The distribution coefficients of the solutes in Case II were seen to increase as the molecular weight of the carboxylic acids increased. As can be seen in Figure 2, the K_D of acetic acid, propionic acid, and butyric acid for the thymol and L-menthol DES was 0.64 ± 0.06 , 2.3 ± 0.06 , and 3.6 ± 0.58 , respectively, and for the TOPO and L-menthol DES it was 2.0 ± 0.29 , 6.2 ± 1.1 , and 6.7 ± 1.7 , respectively. In addition, here, the increasing hydrocarbon carbon backbone decreased the amount of repulsive interaction with hydrophobic DES and allowed for an increase in the distribution coefficient. The values of the thymol and L-menthol DESs were in line with traditional physical solvents, such as n-octanol (e.g., $K_{D,Fur} = 3.2$) [55], methyl isobutyl ketone (e.g., $K_{D,Fur} = 6.9$) [55], and ethyl acetate [21], hence no advancement was seen compared with traditional physical solvents, other than for the application of (a mixture of) biobased chemicals.

The TOPO and L-menthol DES induced overall higher K_D values, which was a consequence of the basic phosphine oxide group and the hydrophobicity of the three alkyl tails. L-lactic acid had a K_D of 0.52 ± 0.07 and 0.40 ± 0.05 for the thymol and L-menthol and TOPO and L-menthol DESs, respectively, which was lower than the propionic acid which contains an equally large hydrocarbon backbone. The additional hydroxyl group of L-lactic acid, not only allows it to interact more strongly with water, but it is also pre-

dominantly present at room temperature as a dimer [71], and was therefore less able to form hydrogen bond bridges with both DESs, which consequently lowered the distribution coefficients. The acetic acid results for TOPO and L-menthol were similar to the TOPO results with other diluents reviewed in [21]. The results were comparable with those for both heptane–hexanol and for a hydrocarbon mixture called Chevron 25, all compared at 45 wt.% TOPO, as reported in [21], which agreed with the 1:3 mol ratio of TOPO to L-menthol. Thus, the application of DESs for the extraction of these biobased chemicals is a method for the utilization of extractants. Without the use of at least one extract either as a hydrogen bond donor or acceptor, the performance of the DES is comparable to traditional physical solvents, while with an extractant as the DES constituent, results similar to the results from traditional diluents may be expected.

4. Conclusions

This work shows the solid–liquid equilibria of type V non-ionic deep eutectic solvents containing thymol and L-menthol, and trioctylphosphine oxide (TOPO) and L-menthol. An equimolar thymol and L-menthol DES and a 1:3 molar ratio of TOPO and L-menthol DES were applied in a liquid–liquid extraction operation in two bio refinery-relevant cases that entailed solutes of formic acid, levulinic acid, furfural, acetic acid, propionic acid, butyric acid, and L-lactic acid. Furfural was extracted to the greatest extent because of its hydrophobic nature. The selectivity between formic acid and levulinic acid could be altered by the choice of DES, as the thymol and L-menthol DES induced a selectivity of levulinic acid over formic acid of $S_{ij} = 9.3 \pm 0.10$, while the TOPO and L-menthol DES induced a selectivity of formic acid over levulinic acid of $S_{ij} = 2.1 \pm 0.28$. The distribution coefficient of the carboxylic acids increased as a function of their molecular weight, which is a measure of the relative apolar regions. L-Lactic acid was extracted more easily than formic acid, because of the larger hydrocarbon backbone; however, it was extracted less than other carboxylic acids because of the water affinity of and dimer formation with the additional hydroxyl function groups.

Author Contributions: Conceptualization, B.S. and T.B.; methodology, B.S. and T.B.; software, T.B.; validation, T.B., B.C.D., J.M.B. and B.S.; formal analysis, T.B., B.C.D., J.M.B., and B.S.; investigation, T.B., B.C.D., J.M.B., and B.S.; resources, B.S.; data curation, T.B.; writing—original draft preparation, T.B.; writing—review and editing, T.B., B.C.D., J.M.B., and B.S.; visualization, T.B. and B.C.D.; supervision, B.S.; project administration, B.S.; funding acquisition, B.S. All authors have read and agreed to the published version of the manuscript.

Funding: This research received no external funding.

Institutional Review Board Statement: Not applicable.

Informed Consent Statement: Not applicable.

Data Availability Statement: All of the data reported in this paper can be requested from the corresponding author.

Acknowledgments: We acknowledge Corbion (Gorinchem, The Netherlands) for supplying the samples of L-lactic acid.

Conflicts of Interest: The authors declare no conflict of interest.

Nomenclature

BP86	Becke and Pedrew functional level of theory
COSMO-RS	Conductor-like screening model for real solvents
Cyrene	Dihydrolevoglucosenone
$\Delta_m H$	Melting enthalpy (kJ mol^{-1})
DES	Deep eutectic solvent
DFT	Density functional theory
Fur	Furfural
γ_i	Activity coefficient of compound i
K_D	Distribution coefficient (-)
LLX	Liquid–liquid extraction
R	Universal gas constant ($8.3145 \text{ J mol}^{-1} \text{ K}^{-1}$)
S_{ij}	Selectivity of compound i over j
SLE	Solid–liquid equilibrium
T	Absolute temperature
T_m	Melting temperature
TOPO	trioctylphosphine oxide
TZVP	triple- ζ valence polarized basis set
x_i	Molar fraction of compound i

References

- Clark, J.H.; Farmer, T.J.; Hunt, A.J.; Sherwood, J. Opportunities for bio-based solvents created as petrochemical and fuel products transition towards renewable resources. *Int. J. Mol. Sci.* **2015**, *16*, 17101–17159. [[CrossRef](#)]
- Brundtland, G.H. Our common future—Call for action. *Environ. Conserv.* **1987**, *14*, 291–294. [[CrossRef](#)]
- Isikgor, F.H.; Becer, C.R. Lignocellulosic biomass: A sustainable platform for the production of bio-based chemicals and polymers. *Polym. Chem.* **2015**, *6*, 4497–4559. [[CrossRef](#)]
- Kang, S.; Fu, J.; Zhang, G. From lignocellulosic biomass to levulinic acid: A review on acid-catalyzed hydrolysis. *Renew. Sustain. Energy Rev.* **2018**, *94*, 340–362. [[CrossRef](#)]
- Ššivec, R.; Grilc, M.; Huš, M.; Likozar, B. Multiscale modeling of (hemi) cellulose hydrolysis and cascade hydrotreatment of 5-hydroxymethylfurfural, furfural, and levulinic acid. *Ind. Eng. Chem. Res.* **2019**, *58*, 16018–16032. [[CrossRef](#)]
- Park, J.-H.; Jin, M.-H.; Lee, D.-W.; Lee, Y.-J.; Song, G.-S.; Park, S.-J.; Namkung, H.; Song, K.H.; Choi, Y.-C. Sustainable low-temperature hydrogen production from lignocellulosic biomass passing through formic acid: Combination of biomass hydrolysis/oxidation and formic acid dehydrogenation. *Environ. Sci. Technol.* **2019**, *53*, 14041–14053. [[CrossRef](#)] [[PubMed](#)]
- Świątek, K.; Gaag, S.; Klier, A.; Kruse, A.; Sauer, J.; Steinbach, D. Acid hydrolysis of lignocellulosic biomass: Sugars and furfurals formation. *Catalysts* **2020**, *10*, 437. [[CrossRef](#)]
- Kucharska, K.; Słupek, E.; Cieśliński, H.; Kamiński, M. Advantageous conditions of saccharification of lignocellulosic biomass for biofuels generation via fermentation processes. *Chem. Pap.* **2020**, *74*, 1199–1209. [[CrossRef](#)]
- Jiménez-Quero, A.; Pollet, E.; Avérous, L.; Phalip, V. Optimized bioproduction of itaconic and fumaric acids based on solid-state fermentation of lignocellulosic biomass. *Molecules* **2020**, *25*, 1070. [[CrossRef](#)]
- Rahmati, S.; Doherty, W.; Dubal, D.P.; Atanda, L.; Moghaddam, L.; Sonar, P.M.; Hessel, V.; Ostrikov, K. Pretreatment and fermentation of lignocellulosic biomass: Reaction mechanisms and process engineering. *React. Chem. Eng.* **2020**, *5*, 2017–2047. [[CrossRef](#)]
- Wu, Y.; Ge, S.; Xia, C.; Mei, C.; Kim, K.-H.; Cai, L.; Smith, L.M.; Lee, J.; Shi, S.Q. Application of intermittent ball milling to enzymatic hydrolysis for efficient conversion of lignocellulosic biomass into glucose. *Renew. Sustain. Energy Rev.* **2021**, *136*, 110442. [[CrossRef](#)]
- Zhang, H.; Han, L.; Dong, H. An insight to pretreatment, enzyme adsorption and enzymatic hydrolysis of lignocellulosic biomass: Experimental and modeling studies. *Renew. Sustain. Energy Rev.* **2021**, *140*, 110758. [[CrossRef](#)]
- Girisuta, B.; Janssen, L.; Heeres, H. Kinetic study on the acid-catalyzed hydrolysis of cellulose to levulinic acid. *Ind. Eng. Chem. Res.* **2007**, *46*, 1696–1708. [[CrossRef](#)]
- Reyhanitash, E.; Zaalberg, B.; Kersten, S.R.; Schuur, B. Extraction of volatile fatty acids from fermented wastewater. *Sep. Purif. Technol.* **2016**, *161*, 61–68. [[CrossRef](#)]
- Ramos-Suarez, M.; Zhang, Y.; Outram, V. Current perspectives on acidogenic fermentation to produce volatile fatty acids from waste. *Rev. Environ. Sci. Bio/Technol.* **2021**, 1–40. [[CrossRef](#)]
- Gössi, A.; Burgener, F.; Kohler, D.; Urso, A.; Kolvenbach, B.A.; Riedl, W.; Schuur, B. In-situ recovery of carboxylic acids from fermentation broths through membrane supported reactive extraction using membrane modules with improved stability. *Sep. Purif. Technol.* **2020**, *241*, 116694. [[CrossRef](#)]
- Da Ros, C.; Conca, V.; Eusebi, A.L.; Frison, N.; Fatone, F. Sieving of municipal wastewater and recovery of bio-based volatile fatty acids at pilot scale. *Water Res.* **2020**, *174*, 115633. [[CrossRef](#)] [[PubMed](#)]

18. Akhtar, J.; Idris, A.; Aziz, R.A. Recent advances in production of succinic acid from lignocellulosic biomass. *Appl. Microbiol. Biotechnol.* **2014**, *98*, 987–1000. [[CrossRef](#)] [[PubMed](#)]
19. Kaur, G.; Garcia-Gonzalez, L.; Elst, K.; Truzzi, F.; Bertin, L.; Kaushik, A.; Balakrishnan, M.; De Wever, H. Reactive extraction for in-situ carboxylate recovery from mixed culture fermentation. *Biochem. Eng. J.* **2020**, *160*, 107641. [[CrossRef](#)]
20. Teke, G.M.; Pott, R.W. Design and evaluation of a continuous semipartition bioreactor for in situ liquid-liquid extractive fermentation. *Biotechnol. Bioeng.* **2021**, *118*, 58–71. [[CrossRef](#)]
21. Sprakel, L.; Schuur, B. Solvent developments for liquid-liquid extraction of carboxylic acids in perspective. *Sep. Purif. Technol.* **2019**, *211*, 935–957. [[CrossRef](#)]
22. Clarke, C.J.; Tu, W.-C.; Levers, O.; Bröhl, A.; Hallett, J.P. Green and sustainable solvents in chemical processes. *Chem. Rev.* **2018**, *118*, 747–800. [[CrossRef](#)] [[PubMed](#)]
23. Paggiola, G.; Van Stempvoort, S.; Bustamante, J.; Barbero, J.M.V.; Hunt, A.J.; Clark, J.H. Can bio-based chemicals meet demand? Global and regional case-study around citrus waste-derived limonene as a solvent for cleaning applications. *Biofuels Bioprod. Biorefining* **2016**, *10*, 686–698. [[CrossRef](#)]
24. Brouwer, T.; Schuur, B. Biobased Entrainer Screening for Extractive Distillation of Acetone and Diisopropyl ether. *Sep. Purif. Technol.* **2021**, *270*, 118749. [[CrossRef](#)]
25. Fegyverneki, D.; Orha, L.; Láng, G.; Horváth, I.T. Gamma-valerolactone-based solvents. *Tetrahedron* **2010**, *66*, 1078–1081. [[CrossRef](#)]
26. Smink, D.; Kersten, S.R.; Schuur, B. Recovery of lignin from deep eutectic solvents by liquid-liquid extraction. *Sep. Purif. Technol.* **2020**, *235*, 116127. [[CrossRef](#)]
27. Brouwer, T.; Schuur, B. Bio-based Solvents as entrainers for Extractive Distillation in Aromatic/Aliphatic and Olefin/Paraffin Separation. *Green Chem.* **2020**, *22*, 5369–5375. [[CrossRef](#)]
28. Brouwer, T.; Schuur, B. Dihydrolevoglucosenone (Cyrene), a Bio-based Solvent for Liquid-Liquid Extraction Applications. *ACS Sustain. Chem. Eng.* **2020**, *8*, 14807–14817. [[CrossRef](#)]
29. Abbott, A.P.; Capper, G.; Davies, D.L.; Rasheed, R.K.; Tambyrajah, V. Novel solvent properties of choline chloride/urea mixtures. *Chem. Commun.* **2003**, *39*, 70–71. [[CrossRef](#)]
30. Abbott, A.P.; Boothby, D.; Capper, G.; Davies, D.L.; Rasheed, R.K. Deep eutectic solvents formed between choline chloride and carboxylic acids: Versatile alternatives to ionic liquids. *J. Am. Chem. Soc.* **2004**, *126*, 9142–9147. [[CrossRef](#)] [[PubMed](#)]
31. Rodríguez, N.R.; González, A.S.; Tijssen, P.M.; Kroon, M.C. Low transition temperature mixtures (LTTMs) as novel entrainers in extractive distillation. *Fluid Phase Equilibria* **2015**, *385*, 72–78. [[CrossRef](#)]
32. Osowska, N.; Ruzik, L. New Potentials in the Extraction of Trace Metal Using Natural Deep Eutectic Solvents (NADES). *Food Anal. Methods* **2019**, *12*, 926–935. [[CrossRef](#)]
33. Oliveira, F.S.; Pereiro, A.B.; Rebelo, L.P.N.; Marrucho, I.M. Deep eutectic solvents as extraction media for azeotropic mixtures. *Green Chem.* **2013**, *15*, 1326–1330. [[CrossRef](#)]
34. Pontes, P.V.; Crespo, E.A.; Martins, M.A.; Silva, L.P.; Neves, C.M.; Maximo, G.J.; Hubinger, M.D.; Batista, E.A.; Pinho, S.P.; Coutinho, J.A.; et al. Measurement and PC-SAFT modeling of solid-liquid equilibrium of deep eutectic solvents of quaternary ammonium chlorides and carboxylic acids. *Fluid Phase Equilibria* **2017**, *448*, 69–80. [[CrossRef](#)]
35. Coutinho, J. Do they exist? And why you should you be concerned about it. In Proceedings of the 4th International Conference on Ionic Liquids in Separation and Purification Technology, Sitges, Spain, 8–11 September 2019.
36. Martins, M.A.; Pinho, S.P.; Coutinho, J.A. Insights into the nature of eutectic and deep eutectic mixtures. *J. Solut. Chem.* **2019**, *48*, 962–982. [[CrossRef](#)]
37. Van Osch, D.J.; Kollau, L.J.B.M.; Bruinhorst, A.A.V.D.; Asikainen, S.; Da Rocha, M.M.A.; Kroon, M.C. Ionic liquids and deep eutectic solvents for lignocellulosic biomass fractionation. *Phys. Chem. Chem. Phys.* **2017**, *19*, 2636–2665. [[CrossRef](#)]
38. Smink, D.; Kersten, S.R.; Schuur, B. Comparing multistage liquid-liquid extraction with cold water precipitation for improvement of lignin recovery from deep eutectic solvents. *Sep. Purif. Technol.* **2020**, *252*, 117395. [[CrossRef](#)]
39. Riveiro, E.; González, B.; Domínguez, Á. Extraction of adipic, levulinic and succinic acids from water using TOPO-based deep eutectic solvents. *Sep. Purif. Technol.* **2020**, *241*, 116692. [[CrossRef](#)]
40. Tang, W.; An, Y.; Row, K.H. Emerging applications of (micro) extraction phase from hydrophilic to hydrophobic deep eutectic solvents: Opportunities and trends. *TrAC Trends Anal. Chem.* **2021**, *136*, 116187. [[CrossRef](#)]
41. Lima, F.; Branco, L.C.; Silvestre, A.J.; Marrucho, I.M. Deep desulfurization of fuels: Are deep eutectic solvents the alternative for ionic liquids? *Fuel* **2021**, *293*, 120297. [[CrossRef](#)]
42. Smith, E.L.; Abbott, A.P.; Ryder, K.S. Deep eutectic solvents (DESs) and their applications. *Chem. Rev.* **2014**, *114*, 11060–11082. [[CrossRef](#)]
43. Chen, Y.; Yu, D.; Chen, W.; Fu, L.; Mu, T. Water absorption by deep eutectic solvents. *Phys. Chem. Chem. Phys.* **2019**, *21*, 2601–2610. [[CrossRef](#)]
44. Van Osch, D.J.; Zubeir, L.F.; Bruinhorst, A.A.V.D.; Da Rocha, M.M.A.; Kroon, M.C. Hydrophobic deep eutectic solvents as water-immiscible extractants. *Green Chem.* **2015**, *17*, 4518–4521. [[CrossRef](#)]
45. Gilmore, M.; McCourt, É.N.; Connolly, F.; Nockemann, P.; Swadźba-Kwaśny, M.; Holbrey, J.D. Hydrophobic deep eutectic solvents incorporating trioctylphosphine oxide: Advanced liquid extractants. *ACS Sustain. Chem. Eng.* **2018**, *6*, 17323–17332. [[CrossRef](#)]

46. Schaeffer, N.; Conceição, J.H.F.; Martins, M.A.R.; Neves, M.C.; Pérez-Sánchez, G.; Gomes, J.R.B.; Papaiconomou, N.; Coutinho, J.A.P. Non-ionic hydrophobic eutectics—versatile solvents for tailored metal separation and valorisation. *Green Chem.* **2020**, *22*, 2810–2820. [[CrossRef](#)]
47. Cañadas, R.; González-Miquel, M.; González, E.J.; Díaz, I.; Rodríguez, M. Hydrophobic eutectic solvents for extraction of natural phenolic antioxidants from winery wastewater. *Sep. Purif. Technol.* **2021**, *254*, 117590. [[CrossRef](#)]
48. Abranches, D.O.; Martins, M.A.R.; Silva, L.P.; Schaeffer, N.; Pinho, S.P.; Coutinho, J.A.P. Phenolic hydrogen bond donors in the formation of non-ionic deep eutectic solvents: The quest for type V DES. *Chem. Commun.* **2019**, *55*, 10253–10256. [[CrossRef](#)] [[PubMed](#)]
49. Florindo, C.; Branco, L.; Marrucho, I. Development of hydrophobic deep eutectic solvents for extraction of pesticides from aqueous environments. *Fluid Phase Equilibria* **2017**, *448*, 135–142. [[CrossRef](#)]
50. Lee, J.; Jung, D.; Park, K. Hydrophobic deep eutectic solvents for the extraction of organic and inorganic analytes from aqueous environments. *TrAC Trends Anal. Chem.* **2019**, *118*, 853–868. [[CrossRef](#)]
51. Van Osch, D.J.; Dietz, C.H.J.T.; Van Spronsen, J.; Kroon, M.C.; Gallucci, F.; Annaland, M.V.S.; Tuinier, R. A search for natural hydrophobic deep eutectic solvents based on natural components. *ACS Sustain. Chem. Eng.* **2019**, *7*, 2933–2942. [[CrossRef](#)]
52. Adeyemi, I.; Sulaiman, R.; Almazroui, M.; Al-Hammadi, A.; AlNashef, I. Removal of chlorophenols from aqueous media with hydrophobic deep eutectic solvents: Experimental study and COSMO RS evaluation. *J. Mol. Liq.* **2020**, *311*, 113180. [[CrossRef](#)]
53. Ribeiro, B.D.; Florindo, C.; Iff, L.C.; Coelho, M.A.Z.; Marrucho, I.M. Menthol-based eutectic mixtures: Hydrophobic low viscosity solvents. *ACS Sustain. Chem. Eng.* **2015**, *3*, 2469–2477. [[CrossRef](#)]
54. Makoš, P.; Przyjazny, A.; Boczkaj, G. Hydrophobic deep eutectic solvents as “green” extraction media for polycyclic aromatic hydrocarbons in aqueous samples. *J. Chromatogr. A* **2018**, *1570*, 28–37. [[CrossRef](#)]
55. Brouwer, T.; Blahusiak, M.; Babic, K.; Schuur, B. Reactive extraction and recovery of levulinic acid, formic acid and furfural from aqueous solutions containing sulphuric acid. *Sep. Purif. Technol.* **2017**, *185*, 186–195. [[CrossRef](#)]
56. Bengtsson, S.; Hallquist, J.; Werker, A.; Welander, T. Acidogenic fermentation of industrial wastewaters: Effects of chemostat retention time and pH on volatile fatty acids production. *Biochem. Eng. J.* **2008**, *40*, 492–499. [[CrossRef](#)]
57. Pham, T.N.; Nam, W.J.; Jeon, Y.J.; Yoon, H.H. Volatile fatty acids production from marine macroalgae by anaerobic fermentation. *Bioresour. Technol.* **2012**, *124*, 500–503. [[CrossRef](#)]
58. Macário, I.P.; Jesus, F.; Pereira, J.L.; Ventura, S.P.; Gonçalves, A.M.; Coutinho, J.A.; Gonçalves, F.J. Unraveling the ecotoxicity of deep eutectic solvents using the mixture toxicity theory. *Chemosphere* **2018**, *212*, 890–897. [[CrossRef](#)] [[PubMed](#)]
59. Ochi, K.; Kato, Y.; Saito, T.; Kurihara, K.; Kojima, K. Determination and correlation of LLE and SLE data for the system aniline+ cyclohexane. *Korean J. Chem. Eng.* **1997**, *14*, 365–368. [[CrossRef](#)]
60. Prausnitz, J.M.; Lichtenthaler, R.N.; De Azevedo, E.G. *Molecular Thermodynamics of Fluid-Phase Equilibria*; Prentice Hall: Hoboken, NJ, USA, 1998; 860p.
61. Coutinho, J.A.; Andersen, S.I.; Stenby, E.H. Evaluation of activity coefficient models in prediction of alkane solid-liquid equilibria. *Fluid Phase Equilibria* **1995**, *103*, 23–40. [[CrossRef](#)]
62. González-Miquel, M.; Díaz, I. Green solvent screening using modelling and simulation. *Curr. Opin. Green Sustain. Chem.* **2021**, *29*, 100469. [[CrossRef](#)]
63. Eckert, F.; Klamt, A. Fast solvent screening via quantum chemistry: COSMO-RS approach. *AIChE J.* **2002**, *48*, 369–385. [[CrossRef](#)]
64. Klamt, A. Conductor-like screening model for real solvents: A new approach to the quantitative calculation of solvation phenomena. *J. Phys. Chem.* **1995**, *99*, 2224–2235. [[CrossRef](#)]
65. Klamt, A. *COSMO-RS: From Quantum Chemistry to Fluid Phase Thermodynamics and Drug Design*; Elsevier: Amsterdam, The Netherlands, 2005; p. 246.
66. Schaeffer, N.; Abranches, D.O.; Silva, L.P.; Martins, M.A.; Carvalho, P.J.; Russina, O.; Triolo, A.; Paccou, L.; Guinet, Y.; Hedoux, A.; et al. Non-Ideality in Thymol+ Menthol Type V Deep Eutectic Solvents. *ACS Sustain. Chem. Eng.* **2021**, *9*, 2203–2211. [[CrossRef](#)]
67. Chen, J.; Brooks, C.L.; Scheraga, H.A. Revisiting the carboxylic acid dimers in aqueous solution: Interplay of hydrogen bonding, hydrophobic interactions, and entropy. *J. Phys. Chem. B* **2008**, *112*, 242–249. [[CrossRef](#)] [[PubMed](#)]
68. Pei, Y.; Wu, K.; Wang, J.; Fan, J. Recovery of furfural from aqueous solution by ionic liquid based liquid–liquid extraction. *Sep. Sci. Technol.* **2008**, *43*, 2090–2102. [[CrossRef](#)]
69. Habbal, S.; Haddou, B.; Kameche, M.; Derriche, Z.; Canselier, J.; Gourdon, C. Cloud point or ionic liquid extraction of furfural from aqueous solution: A comparative study based upon experimental design. *Desalination Water Treat.* **2016**, *57*, 23770–23778. [[CrossRef](#)]
70. Xin, K.; Song, Y.; Dai, F.; Yu, Y.; Li, Q. Liquid–liquid equilibria for the extraction of furfural from aqueous solution using different solvents. *Fluid Phase Equilibria* **2016**, *425*, 393–401. [[CrossRef](#)]
71. Losada, M.; Tran, H.; Xu, Y. Lactic acid in solution: Investigations of lactic acid self-aggregation and hydrogen bonding interactions with water and methanol using vibrational absorption and vibrational circular dichroism spectroscopies. *J. Chem. Phys.* **2008**, *128*, 014508. [[CrossRef](#)]